**Electronic Spectroscopy and Electrochemistry.** $Mo_2Cl_6(dppe)_2$ was studied by UV–visible spectroscopy in $CH_2Cl_2$ solution. Characteristic spectral features are as follows ($\lambda_{max}$, nm ($\epsilon$)): 232 (122 000), 310 (7200), 392 (380), and 507 (2050).

A cyclic voltammogram of **1** in 0.2 M TBAH in $CH_2Cl_2$, available as supplementary material, revealed one irreversible reduction wave at $E_{1/2} = -1.10$ V and two reversible one-electron oxidations at $E_{1/2} = +1.45$ V and $E_{1/2} = +0.85$ V vs Ag/AgCl. For these couples, the $i_{p,a}/i_{p,c}$ ratios were close to unity and the separation ($\Delta E_p$) between the anodic and cathodic peaks was ~65 mV at a scan rate of 200 mV/s. The oxidations correspond to the processes $Mo^{III}Mo^{III} - e^- \rightarrow Mo^{III}Mo^{IV}$ and $Mo^{III}Mo^{IV} - e^- \rightarrow Mo^{IV}Mo^{IV}$.

In contrast to the above redox chemistry, the cyclic voltammogram of the quadruply bonded $\beta$-$Mo_2Cl_4(dppe)_2$[22] consists of only one accessible oxidation ($Mo^{II}Mo^{II} - e^- \rightarrow Mo^{II}Mo^{III}$), attesting to the stability of the $\sigma^2\pi^4\delta^2$ configuration.

**Concluding Remarks.** We have demonstrated that the quadruple bonds of dimolybdenum and ditungsten undergo facile oxidative addition reactions with $Cl_2$. The reactions can be controlled to produce the desired $M_2^{6+}$ compounds in high yield.

The isolation and structural characterization of the complexes $Mo_2Cl_6(dedppe)_2$ and $M_2Cl_6(dppe)_2$ (M = Mo, W) increases our gallery of $M_2L_{10}$ compounds possessing an edge-sharing bioctahedral geometry. The dppe compounds are particularly interesting because they belong to a homologous series that now includes examples with the metals Zr, Nb, Ta, Mo, W, and Re. We hope to be able to prepare the Tc, Ru, and Os analogues as well.

One interesting aspect of the structures reported here is that the $M_2Cl_6(dppe)_2$ molecules, in which the diphosphine ligands could not be supposed to play any role in tying the metal atoms together, have approximately the same M–M distances as those found in the $M_2Cl_6(dppm)_2$ molecules,[23] where such a role might be postulated. Thus, we have the following comparisons of M–M distances, in Å:

| | | | |
|---|---|---|---|
| $Mo_2Cl_6(dppm)_2$ | 2.789 (1) | $Mo_2Cl_6(dppe)_2$ | 2.762 (1) |
| $W_2Cl_6(dppm)_2$ | 2.691 (1) | $W_2Cl_6(dppe)_2$ | 2.682 (1) |

In fact, to the extent that differences exist between dppm and dppe compounds with the same metal atom, it is the former which have the longer M–M bonds.

Another notable point is that the tendency of the W–W bonds to be ca. 0.10 Å shorter than analogous Mo–Mo bonds seems to be independent of the exact arrangement of the ligands, that is, whether the diphosphines bridge axial positions or chelate in the equatorial plane.

**Acknowledgment.** We thank the National Science Foundation for support.

**Registry No.** **1**, 110900-34-0; **2**, 110717-87-8; **3**, 110717-89-0; $Mo_2Cl_6(dppe)_2$, 92479-08-8; $W_2Cl_6(dppe)_2$, 110717-88-9; $\beta$-$Mo_2Cl_4(dppe)_2$, 64508-32-3; $\alpha$-$Mo_2Cl_4(dppe)_2$, 64490-77-3; $Mo_2Cl_4(dedppe)_2$, 110373-57-4; $\alpha$-$W_2Cl_4(dppe)_2$, 86782-93-6; $\beta$-$W_2Cl_4(dppe)_2$, 73133-24-1; $Mo_2Cl_6(dppe)_2^+$, 110717-90-3; $Mo_2Cl_6(dppe)_2^{2+}$, 110717-91-4; $CH_2Cl_2$, 75-09-2; Mo, 7439-98-7; W, 7440-33-7; chlorine, 7782-50-5.

**Supplementary Material Available:** A listing of positional parameters for phenyl group atoms in **3** (Table IVS), full listings of bond angles, bond distances, and anisotropic displacement parameters for **1–3**, listings of molar magnetic susceptibility data for **1** and **3**, and a figure depicting the cyclic voltammogram of **3** (22 pages); tables of observed and calculated structure factors for **1–3** (50 pages). Ordering information is given on any current masthead page.

(22) Zietlow, T. C.; Klendworth, D. D.; Nimry, T.; Salmon, D. J.; Walton, R. A. *Inorg. Chem.* **1981**, *20*, 947.

(23) Canich, J. M.; Cotton, F. A.; Daniels, L. M.; Lewis, D. B. *Inorg. Chem.*, in press.

Contribution from the School of Chemistry,
University of New South Wales, Kensington, NSW 2033, Australia

# The Different Nonmolecular Polyadamantanoid Crystal Structures of $Cd(SPh)_2$ and $Cd(SC_6H_4Me\text{-}4)_2$. Analogies with Microporous Aluminosilicate Frameworks[1]

Ian G. Dance,* Robert G. Garbutt, Donald C. Craig, and Marcia L. Scudder

*Received March 3, 1987*

$Cd(SPh)_2$ (**2**) crystallizes unsolvated from DMF with a structure (orthorhombic, $P2_12_12_1$, $a = 15.490$ (2) Å, $b = 15.626$ (2) Å, $c = 20.803$ (3) Å, $Z = 16$ ($CdS_2C_{12}H_{10}$), 3626 observed data, Mo K$\alpha$, $R = 0.034$) in which adamantanoid cages comprised of four Cd atoms and six doubly bridging SPh ligands are connected in three dimensions by doubly bridging SPh ligands. The lattice arrangement of the linked tetrahedral adamantanoid cages is almost identical with that of the $\alpha$-cristobalite form of $SiO_2$. The structure of crystalline $Cd(SC_6H_4Me\text{-}4)_2$ (**3**) (monoclinic, $P2_1/c$, $a = 27.196$ (9) Å, $b = 15.722$ (5) Å, $c = 37.046$ (13) Å, $\beta = 132.03$ (1)°, $Z = 32$ ($CdS_2C_{14}H_{14}$), 12 003 observed data with $(\sin\theta)/\lambda > 0.1$ Å$^{-1}$, Mo K$\alpha$, $R = 0.065$) is also three-dimensionally nonmolecular with vertex-linked adamantanoid tetrahedra, but in a very different linkage pattern involving closed four-, six-, and eight-membered rings of tetrahedra, resembling microporous zeolite lattices. In **3** there exist very large centrosymmetric cavities in the Cd,S array, surrounded by 12 adamantanoid cages whose centroids constitute a trans truncated octahedron. Channels encycled by eight-membered rings also exist in the lattice. The cavities are lined with 44 S atoms connected by 32 Cd atoms, contain 10 ligand substituents, and are connected through four- and six-membered rings to other cavities. Within the cavities the S---S diagonals through the inversion center range from 16.6 to 19.1 Å. The volumes excluded by the Cd,S cores of the adamantanoid tetrahedra are 12% and 10% of the unit cell volumes in **2** and **3**, respectively, and the remaining volumes occupied by the substituents are partially empty. Both of these poly-linked-adamantanoid structures are unique.

## Introduction

Although the chemistry of anionic polymetallic thiolate complexes $[M_x(SR)_y]^{z-}$ has been developed quite extensively, at least for some metals, fundamental knowledge of the structures of the uncharged metal thiolates $[M(SR)_n]_p$ is relatively sparse.[2] This is due in part to the relative insolubility of the uncharged compounds in inert solvents, attributed to structural nonmolecularity in the crystal phase, and the consequent problem of obtaining crystals of diffraction quality.

We are concerned here with the structural chemistry of the set of compounds $M(SR)_2$ (R noncoordinating) in which M is tet-

(1) Previous paper in this series on polycadmium complexes: Dance, I. G.; Garbutt, R.; Craig, D. C. *Inorg. Chem.* **1987**, *26*, 3732.

(2) Dance, I. G. *Polyhedron* **1986**, *5*, 1037.

0020-1669/87/1326-4057$01.50/0 

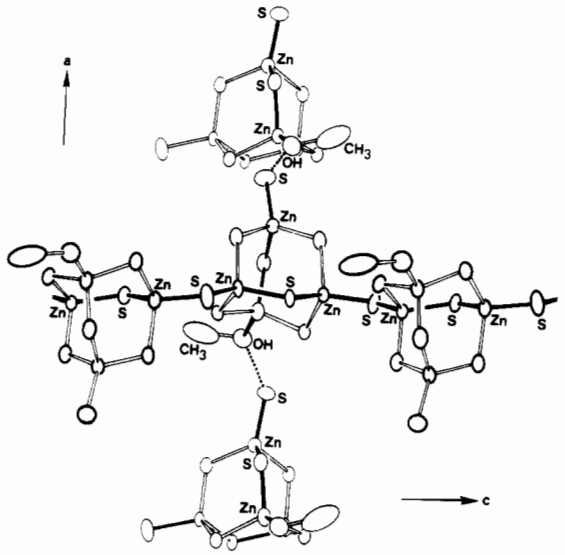


**Figure 1.** Crystal structure of $Zn_4(SPh)_8MeOH$ (**1**).

rahedrally coordinated, specifically M = Zn, Cd, although the principles developed should be transferable to other tetrahedral $M^{2+}$. Crystal structures are known for two compounds $Cd(SR)_2$, where R contains additional donor functions: $Cd(\mu\text{-}SCH_2COOEt)_2$ is one-dimensionally nonmolecular,[3] and $Cd(\mu\text{-}SCH_2CH_2OH)_2$ is two-dimensionally nonmolecular.[4] Both of these compounds involve some additional coordination by nonthiolate functions. The most relevant previous study with arenethiolate ligands is that of the $Zn(SPh)_2$ system,[5] where soluble species can be obtained in acetone and thermal polymerization occurs in the presence of small alcohols to form one-dimensionally nonmolecular crystalline compounds $Zn_4(SPh)_8(ROH)$ (**1**). The crystal structure of **1** (R = Me), shown in Figure 1, contains adamantanoid cages [*octahedro*-($\mu$-$SPh)_6$-*tetrahedro*-$Zn_4$] linked along $2_1$ axes parallel to *c* by doubly bridging $PhS^-$ ligands, with terminal $PhS^-$ and MeOH ligands at the other two Zn atoms, i.e. $^1_\infty[(\mu\text{-}SPh)_6Zn_4(\mu\text{-}SPh)_{2/2}(SPh)(MeOH)]$. A metastable solution of **1** can be obtained in the relatively inert solvent acetonitrile, but no information is available on the structures of the depolymerized dissolved species.

The structure of **1**, and the ubiquity of the adamantanoid cage moiety,[2] prompted the suggestion of a two-dimensionally nonmolecular structure of unsolvated $M(SAr)_2$, comprised of adamantanoid cages linked in two directions by doubly bridging thiolates, i.e. $^2_\infty[(\mu\text{-}SAr)_6M_4(\mu\text{-}SAr)_{4/2}]$.[2] We report here the crystal structures of $Cd(SPh)_2$ (**2**) and of $Cd(SC_6H_4Me\text{-}4)_2$ (**3**), two different *three*-dimensionally nonmolecular structures with adamantanoid cages linked by thiolate bridges. The arrangement of vertex-linked adamantanoid tetrahedra in **2** is that of $\alpha$-cristobalite, while the arrangement in **3** contains open cavities connected through four-, six-, and eight-membered rings of tetrahedra, as in aluminosilicate structures. These results have been communicated briefly.[6,7]

## Experimental Section

**Preparations and Crystallizations. $Cd(SPh)_2$ (2).** $Cd(NO_3)_2.4H_2O$ (36.6 g, 0.118 mol) in methanol (50 mL) was added slowly to a well-stirred solution of benzenethiol (26.7 g, 0.242 mol) and triethylamine (24.0 g, 0.237 mol) in methanol, in the absence of oxygen. The white microcrystalline precipitate was filtered, washed thoroughly with methanol and acetone, and vacuum dried. Further purification was by reprecipitation from DMF by using water. Mp: 339–344 °C dec. Anal. Calcd for $CdS_2C_{12}H_{10}$: C, 43.58; H, 3.05. Found: C, 43.48; H, 2.89. Crystals were grown by layering ethanol (8 mL) over a solution of solid **2** (0.3 g) in DMF (1 mL). After 4 days the blocky crystals had grown up to 2-mm dimensions. Acetone or acetonitrile can also be used as precipitant. **2** is insoluble in all common solvents except DMF (solubility 1.2 g/mL at 25 °C, 1.35 g/mL at 60 °C) and DMSO (0.76 g/mL at 20 °C).

The same crystalline form of **2** was obtained by other standard methods, including reaction of $CdCO_3$ or $Cd(OAc)_2$ with benzenethiol in methanol at high and low temperatures, and reaction of $Cd(NO_3)_2$ with benzenethiol plus triethylamine in methanol. Polycrystalline diffraction data for **2** and **3** are included in the supplementary material.[8]

**$Cd(SC_6H_4Me\text{-}4)_2$ (3)** was prepared by the procedure for **2**. Anal. Calcd for $CdS_2C_{14}H_{14}$: C, 46.87; H, 3.93. Found: C, 46.74; H, 3.99. Mp: 285 °C dec. Crystals of up to 2-mm dimension were grown by the same method from a 0.25 g/mL solution in DMF. The solubility of **3** in DMF is 0.75 g/mL at 27 °C and 1.10 g/mL at 85 °C, and in DMSO is 0.65 g/mL at 20 °C.

**Crystal Structure Determinations.** The crystal structures were determined by standard procedures, on an Enraf Nonius CAD4 diffractometer, with monochromatized Mo K$\alpha$ radiation. Data collection, reduction, and absorption corrections were carried out according to procedures previously described.[9] Weights $w = 1/\sigma^2(F_o)$ were assigned to reflections, with $\sigma(F_o)$ being derived from $\sigma(I_o) = [\sigma(I_o) + (0.04I_o)^2]^{1/2}$. Corrections were made for the small amount of decay of crystalline **3**. No corrections were made for extinction. Details of the crystal lattices, the intensity collection, and the final refinement are contained in Table I. Structure **2** has one adamantanoid cage moiety, $[(\mu\text{-}SPh)_6Cd_4(\mu\text{-}SPh)_2]$, per crystallographic asymmetric unit, while in **3** there are two such cages, labeled A and B, in the asymmetric unit. Atom labeling is defined in Figure 2, which shows the details of the crystallographically independent adamantanoid tetrahedra. The structure solutions used direct methods (MULTAN). Refinements of the structures initially used standard least squares, but in each case the refinement was completed with a constrained refinement program (RAELS)[10] with facility for rigid group refinement. Scattering factors, including real and imaginary anomalous scattering by Cd and S, were from ref 11. Details of each refinement follow.

**Table I.** Details of the Crystallographic Analyses

| | **2** | **3** |
|---|---|---|
| formula | $C_{12}H_{10}CdS_2$ | $C_{14}H_{14}CdS_2$ |
| formula mass | 330.73 | 358.79 |
| cryst descrpn | *c'* less prisms | *c'* less prisms |
| space group | $P2_12_12_1$ | $P2_1/c$ |
| *a*, Å | 15.490 (2) | 27.196 (9) |
| *b*, Å | 15.626 (2) | 15.722 (5) |
| *c*, Å | 20.803 (3) | 37.046 (13) |
| $\beta$, deg | 90 | 132.03 (1) |
| V, Å$^3$ | 5035 (1) | 11767 (7) |
| temp, °C | 21 (1) | 21 (1) |
| $d_{obsd}$, g cm$^{-3}$ | 1.74 | 1.61 |
| *Z* | 16 | 16 |
| $d_{calcd}$, g cm$^{-3}$ | 1.74 | 1.62 |
| radiation; $\lambda$, Å | Mo K$\alpha$; 0.7107 | Mo K$\alpha$; 0.7107 |
| $\mu$, cm$^{-1}$ | 20.13 | 17.29 |
| cryst dimens, mm | 0.10 × 0.10 × 0.18 | 0.15 × 0.22 × 0.14 |
| scan mode | $\theta/2\theta$ | $\theta/2\theta$ |
| $2\theta_{max}$, deg | 50 | 40 |
| no. of intens measmts | 4884 | 17431 |
| criterion for obsd reflcn | $I/\sigma(I) > 3$ | $I/\sigma(I) > 3$ |
| no. of indep obsd reflcns | 3626 | 12107 |
| no. of reflcns (*m*) and variables (*n*) in final refinement | 3626, 238 | 12003, 464 |
| $R = \sum^m\|\Delta F\|/\sum^m\|F_o\|$ | 0.034 | 0.065 |
| $R_w = [\sum^m w\|\Delta F\|^2/\sum^m w\|F_o\|^2]^{1/2}$ | 0.039 | 0.085 |
| $s = [\sum^m w\|\Delta F\|^2/(m-n)]^{1/2}$ | 1.18 | 2.98 |
| cryst decay | none | 1–0.85 |
| max, min transmission coeff | 0.83, 0.65 | 0.78, 0.64 |
| merging *R*, for *n* reflcns measd twice | | 0.032, 307 |

(3) Dance, I. G.; Scudder, M. L.; Secomb, R. *Inorg. Chem.* **1983**, *22*, 1794.
(4) Burgi, H. B. *Helv. Chim. Acta* **1974**, *57*, 513.
(5) Dance, I. G. *J. Am. Chem. Soc.* **1980**, *102*, 3445.
(6) Craig, D.; Dance, I. G.; Garbutt, R. *Angew. Chem., Int. Ed. Engl.* **1986**, *25*, 165.
(7) Dance, I. G.; Garbutt, R. G.; Craig, D. C.; Scudder, M. L.; Bailey, T. D. *J. Chem. Soc., Chem. Commun.* **1987**, 1164.
(8) See paragraph at end of paper regarding supplementary material.
(9) Dance, I. G.; Guerney, P. J.; Rae, A. D.; Scudder, M. L. *Inorg. Chem.* **1983**, *22*, 2883.
(10) Rae, A. D. "RAELS, A Comprehensive Constrained Least-Squares Refinement Program"; University of New South Wales, 1984.
(11) Ibers, J. A., Hamilton, W. C., Eds. *International Tables for X-Ray Crystallography*; Kynoch Press: Birmingham, England, 1974; Vol. 4, Tables 2.2A and 2.3.1.

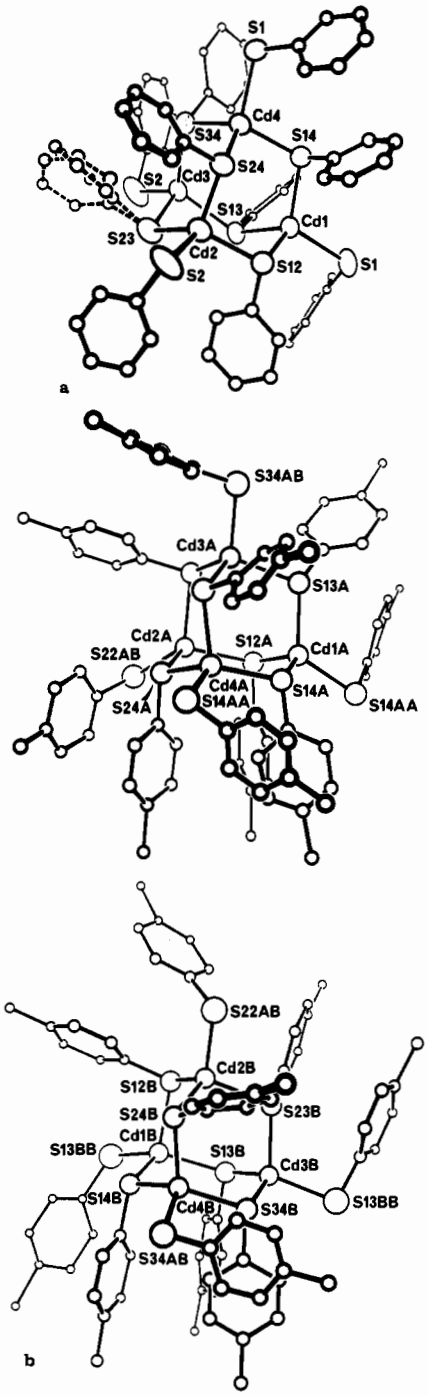


**Figure 2.** Comparable views of (a) the adamantanoid cage in **2** and (b) the two independent adamantanoid cages in **3**. Thermal ellipsoids are drawn at the 50% probability level.

**Structure 2.** Each benzenethiolate ligand was refined by using local coordinates defined relative to its own orthonormal axial system. Six variables per ligand refined the position and orientation of the local axial system, and a common set of local coordinates for C and H atoms was refined so as to maintain *mm*2 symmetry and conserve CH distances and orientation. The S atoms were included in the local *mm*2 symmetry, but two sets of ligands were distinguished for inter- and intracage bridging ligands and were allowed separately refined S–C(1) distances. The difference between the two S–C(1) distances was 0.004 (5) Å and was insignificant. The apparent shortening of the C(1)–C(2) and C(3)–C(4) (and C(1)–C(6), C(4)–C(5)) bonds of the phenyl ring relative to the other two bonds of the ring is consistent with observed dominant libration components about the S–C···C axis of each group. One ligand (labeled 23) was, in fact, found to be disordered and treated as two different rings of equal occupancy (see Figure 2). The thermal parameters for each phenyl group were a 12-parameter **TL** model (where **T** is the translational tensor and **L** the librational tensor) with the origin fixed on the appropriate S atom. The Cd and S atoms were refined as anisotropic atoms in the normal way. The final residual was 0.034 for 3626 observed reflections (0.036 for the other enantiomer), and the largest peak in the final difference map was 0.74 e Å$^{-3}$. The low value of the final residual demonstrates the physical reliability of the constraints imposed in the refinement.

**Table II.** Fractional Coordinates for Cd, S, and $C_\alpha$ atoms of **2**

| atom | *x* | *y* | *z* |
|---|---|---|---|
| Cd(1) | 0.27598 (4) | 0.23280 (4) | 0.40455 (3) |
| Cd(2) | 0.46685 (5) | 0.31887 (4) | 0.27997 (3) |
| Cd(3) | 0.47313 (5) | 0.06939 (4) | 0.33993 (3) |
| Cd(4) | 0.53444 (5) | 0.26579 (4) | 0.46301 (3) |
| S(1) | 0.1162 (2) | 0.2291 (2) | 0.4316 (1) |
| S(2) | 0.5110 (3) | 0.4126 (2) | 0.1871 (1) |
| S(12) | 0.3093 (2) | 0.3369 (2) | 0.3128 (1) |
| S(13) | 0.3116 (2) | 0.0895 (1) | 0.3547 (1) |
| S(14) | 0.3760 (2) | 0.2702 (2) | 0.4969 (1) |
| S(23) | 0.4992 (2) | 0.1666 (2) | 0.2436 (1) |
| S(24) | 0.5464 (2) | 0.3802 (2) | 0.3774 (1) |
| S(34) | 0.5805 (2) | 0.1200 (2) | 0.4220 (1) |
| C(11) | 0.0795 (2) | 0.1381 (4) | 0.3893 (3) |
| C(12) | 0.4860 (3) | 0.3585 (2) | 0.1148 (2) |
| C(112) | 0.2425 (3) | 0.2989 (3) | 0.2500 (2) |
| C(113) | 0.2759 (2) | 0.0086 (2) | 0.4080 (2) |
| C(114) | 0.3547 (2) | 0.3783 (3) | 0.5171 (2) |
| C(123) | 0.6132 (3) | 0.1599 (7) | 0.2401 (4) |
| C(123′)[a] | 0.6114 (3) | 0.1560 (7) | 0.2297 (4) |
| C(124) | 0.6554 (3) | 0.3971 (2) | 0.3550 (1) |
| C(134) | 0.5634 (2) | 0.0619 (2) | 0.4940 (2) |

[a] C(123) and C(123′) are alternate positions refined with equal occupancy.

**Structure 3.** As in **2** each ligand was treated and refined as a group of *mm*2 symmetry. Once again, the refinement of a global model for the ring led to slight decreases in the C(1)–C(2) and C(3)–C(4) (and C(1)–C(6), C(4)–C(5)) bond lengths when compared to the other two bonds. As for **2** the difference in the global S–C(1) distances for inter- and intracage bridges was not significant (0.003 (4) Å). For economy of computation, the 112 hydrogen atoms were excluded from the refinement. Consequently, 104 reflections with $(\sin\theta)/\lambda < 0.1$ (for which $R = 0.10$) were omitted from the calculation of derivatives, as these data are most susceptible to the omitted atoms. The thermal parameters for the 16 independent PhMe groups were refined by using a 12-parameter **TL** model for each, with the origin on the appropriate S atom. Cd and S were refined as individual anisotropic atoms. The final residual for 12003 reflections was 0.065, and the largest peak in the final difference map was 0.46 e Å$^{-3}$. Atomic coordinates for both structures are listed in Tables II and III. Thermal parameters and complete listings of dimensions are deposited.[8]

## Results

**Preparation of Crystalline Compounds.** $Cd(SPh)_2$ (**2**) and $Cd(SC_6H_4Me\text{-}4)_2$ (**3**) were each obtained in one unsolvated crystalline form by different crystallization and precipitation methods. Both compounds are strongly soluble in DMF and DMSO, but quite insoluble in other inert solvents, and can be grown as large single crystals from mixtures of DMF and other liquids.[12] **2** and **3** dissolve by reaction with coordinating amines, and crystallize as amine adducts.[13] Attempts to crystallize a cadmium analogue of $Zn_4(SPh)_8(MeOH)$ (**1**) have yielded only **2**, and attempts to crystallize **1** in the lattice of **2** have yielded only an oil.

**Crystal Structure of $Cd(SPh)_2$ (2).** The structural unit in crystalline $Cd(SPh)_2$ (**2**) is the adamantanoid cage shown in full in Figure 2. Each cage is linked to four other cages by bridging through terminal thiolates, and so all thiolate ligands are doubly bridging. All Cd–S bonds are of approximately equal length, and all Cd atoms have tetrahedral primary coordination only (for details, see below): the structural formulation of the compound is $^3_\infty[(\mu\text{-}SPh)_6Cd_4(\mu\text{-}SPh)_{4/2}]$. Figure 3 shows the linkage pattern of the adamantanoid cages, relative to the elements of the orthorhombic space group $P2_12_12_1$ of the crystal. The four linkages

(12) The solubility of $Cd(SPh)_2$ in DMF has been noted previously: Barabash, Y. V.; Skrypnik, Y. G.; Shevchuk, I. A.; Korotkova, Z. G. *J. Anal. Chem. USSR* (Engl. Transl.) **1979**, *34*, 1163.
(13) Dance, I. G.; Hillier, G.; Scudder, M. L., in preparation.

**Table III.** Fractional Coordinates for Cd, S, and $C_a$ atoms of **3**

| atom | *x* | *y* | *z* |
|---|---|---|---|
| Cd(1A) | 0.49551 (4) | 0.62298 (5) | 0.69652 (3) |
| Cd(2A) | 0.58710 (4) | 0.43974 (5) | 0.67840 (3) |
| Cd(3A) | 0.38325 (4) | 0.46408 (5) | 0.57467 (3) |
| Cd(4A) | 0.46854 (4) | 0.37095 (5) | 0.70968 (3) |
| S(12A) | 0.5900 (1) | 0.5956 (2) | 0.6985 (1) |
| S(13A) | 0.3847 (1) | 0.6048 (2) | 0.6093 (1) |
| S(14A) | 0.4617 (1) | 0.5213 (2) | 0.7306 (1) |
| S(23A) | 0.4872 (1) | 0.4484 (2) | 0.5879 (1) |
| S(24A) | 0.5605 (1) | 0.3276 (2) | 0.7128 (1) |
| S(34A) | 0.3725 (1) | 0.3509 (2) | 0.6178 (1) |
| S(14AA) | 0.5407 (2) | 0.7610 (2) | 0.7448 (1) |
| S(22AB) | 0.6966 (2) | 0.3829 (2) | 0.7082 (1) |
| S(34AB) | 0.2777 (2) | 0.4657 (2) | 0.4861 (1) |
| Cd(1B) | 0.08853 (4) | 0.73231 (5) | 0.30633 (3) |
| Cd(2B) | 0.22366 (4) | 0.61431 (5) | 0.30518 (3) |
| Cd(3B) | 0.05052 (4) | 0.48630 (5) | 0.25913 (3) |
| Cd(4B) | 0.21743 (4) | 0.53865 (5) | 0.40457 (3) |
| S(12B) | 0.1535 (1) | 0.7445 (2) | 0.2791 (1) |
| S(13B) | −0.0031 (1) | 0.6314 (2) | 0.2418 (1) |
| S(14B) | 0.1728 (1) | 0.6882 (2) | 0.3949 (1) |
| S(23B) | 0.1317 (1) | 0.5068 (2) | 0.2463 (1) |
| S(24B) | 0.2974 (1) | 0.5758 (2) | 0.3942 (1) |
| S(34B) | 0.1318 (1 | 0.4271 (2) | 0.3447 (1) |
| S(13BB) | 0.0388 (2) | 0.8761 (2) | 0.2991 (1) |
| C(112A) | 0.6668 (2) | 0.6075 (2) | 0.7595 (2) |
| C(113A) | 0.3632 (2) | 0.6846 (2) | 0.5665 (1) |
| C(114A) | 0.5260 (2) | 0.5410 (2) | 0.7942 (1) |
| C(123A) | 0.4901 (2) | 0.3484 (2) | 0.5666 (1) |
| C(124A) | 0.6325 (2) | 0.3218 (2) | 0.7760 (1) |
| C(134A) | 0.3001 (2) | 0.3708 (2) | 0.6086 (1) |
| C(114AA) | 0.5389 (2) | 0.8264 (2) | 0.7044 (2) |
| C(122AB) | 0.7049 (2) | 0.2814 (3) | 0.7336 (2) |
| C(134AB) | 0.2525 (2) | 0.3589 (3) | 0.4642 (1) |
| C(112B) | 0.2026 (2) | 0.8378 (2) | 0.3094 (1) |
| C(113B) | −0.0601 (2) | 0.6378 (2) | 0.2506 (1) |
| C(114B) | 0.1390 (2) | 0.6720 (2) | 0.4223 (1) |
| C(123B) | 0.0921 (2) | 0.5515 (2) | 0.1881 (1) |
| C(124B) | 0.3374 (2) | 0.4817 (2) | 0.3980 (1) |
| C(134B) | 0.0795 (2) | 0.4087 (2) | 0.3571 (1) |
| C(113BB) | 0.0410 (2) | 0.8825 (2) | 0.3484 (2) |

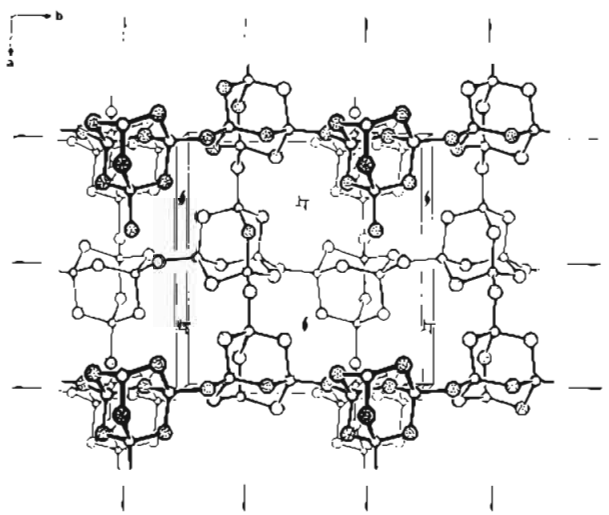


**Figure 3.** Polyadamantanoid cage framework in crystalline **2**, drawn with all phenyl groups omitted. The larger dotted circles are the sulfur atoms. The view direction is tilted 3° from *c*. The open $4_3$ symbols signify pseudo-$4_3$ axes (exact $2_1$ axes) in this pseudo $P4_32_12$ structure; other symmetry elements of the exact space group $P2_12_12_1$ are marked. The $2_1$ axes parallel to *b* are at $z = {}^1/_4$.

at each cage occur along the $2_1$ axes (straddled by the cages) parallel to the *a* and *b* crystal axes. In the third orthogonal direction the cages surround rather than straddle the $2_1$ axes, and are connected in fourfold helical sequences about pseudo-$4_3$ (actual $2_1$) axes, which are marked on Figure 3. These helical connections and the consequent interweaving of the chains parallel to *a* and *b* complete the achievement of the three-dimensional nonmolecularity. The Cd,S atom set approaches the symmetry of space group $P4_32_12$; the correspondence requires interchange of axes *a* and *c*.

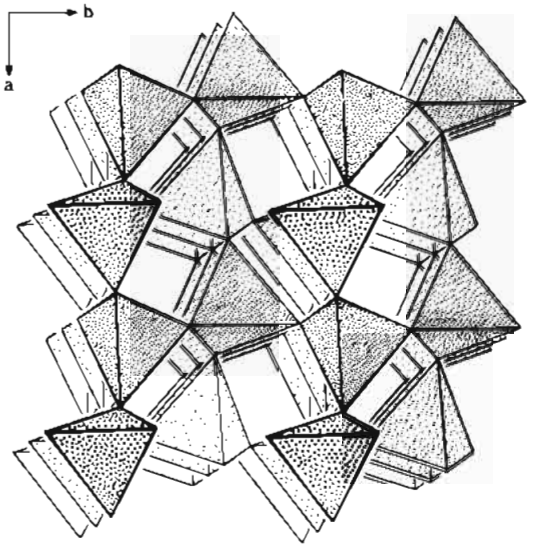


**Figure 4.** Linkage pattern of the adamantanoid tetrahedra of **2**. The view direction is the same as that of Figure 3.

An alternative and simpler presentation of the crystal structure is based on the fact that the $S_{10}$ atom set of the adamantanoid cage constitutes a large tetrahedron (edge-centered by the intracage-bridging S atoms), and consequently the linked adamantanoid cages can be represented by vertex-linked tetrahedra. Figure 4 shows this representation, which reveals that the structure is topologically homologous to that of the $\alpha$-cristobalite form of $SiO_2$ (space group $P4_32_12$), in which the tetrahedra are simply the $SiO_4$ coordination tetrahedra. Clearly there is a large difference in scale between the two structures, since eight independent phenyl substituents per tetrahedron must be accommodated in **2**, but the difference in orientation of the tetrahedra is minimal. Rotation of the tetrahedra is a degree of freedom in the $\alpha$-cristobalite structure type, affecting the intertetrahedra angles,[14] but the Si–O–Si angle in $\alpha$-cristobalite, 146.4°, and the mean intercage Cd–S–Cd angle in **2**, 136.1°, are similar. Further geometrical details and the locations of substituents in the crystal lattice are described below in conjunction with the results for **3**.

**Crystal Structure of $Cd(SC_6H_4CH_3\text{-}4)_2$ (3).** This compound also contains adamantanoid cage units, linked to four neighbors by doubly bridging thiolate ligands in a three-dimensionally nonmolecular lattice, and can be formulated as $^3_\infty[(\mu\text{-}SC_6H_4CH_3)_6Cd_4(\mu\text{-}SC_6H_4CH_3)_{4/2}]$. However the cage connectivity pattern and the lattice symmetry are quite different from those of **2**. The crystal space group is monoclinic $P2_1/c$, but with $\beta$ (132.0°) close to 90 + 45° and $c(\sin\beta)$ (27.53 Å) $\approx a$ (27.20 Å) such that there is a pseudo square array of $2_1$ axes and inversion centers projected along *b*.

Again the description of the lattice is in terms of adamantanoid tetrahedra sharing vertices, but in **3** the tetrahedra are linked in closed cycles, not helices. Four-, six-, and eight-membered rings of adamantanoid tetrahedra occur, and the lattice contains a larger structural feature that is a polyhedral cavity, with the faces formed by four- and six-membered rings. The occurrence of vertex-linked tetrahedra in cycles and their enclosure of polyhedral cavities (and channels, see below), are features characteristic of the three-dimensional aluminosilicate (zeolite) structures, which **3** resembles. Figure 5 shows one cavity, presented in terms of (a) the Cd and S atoms, (b) the 12 adamantanoid cage tetrahedra that surround the cavity, and (c) the 12-vertex decahedron formed by the connected centroids of the tetrahedra. There are two crystallographically independent adamantanoid cages, A and B, with

(14) O'Keefe, M.; Hyde, B. G. *Acta Cryst.* **1976**, *B32*, 2923.

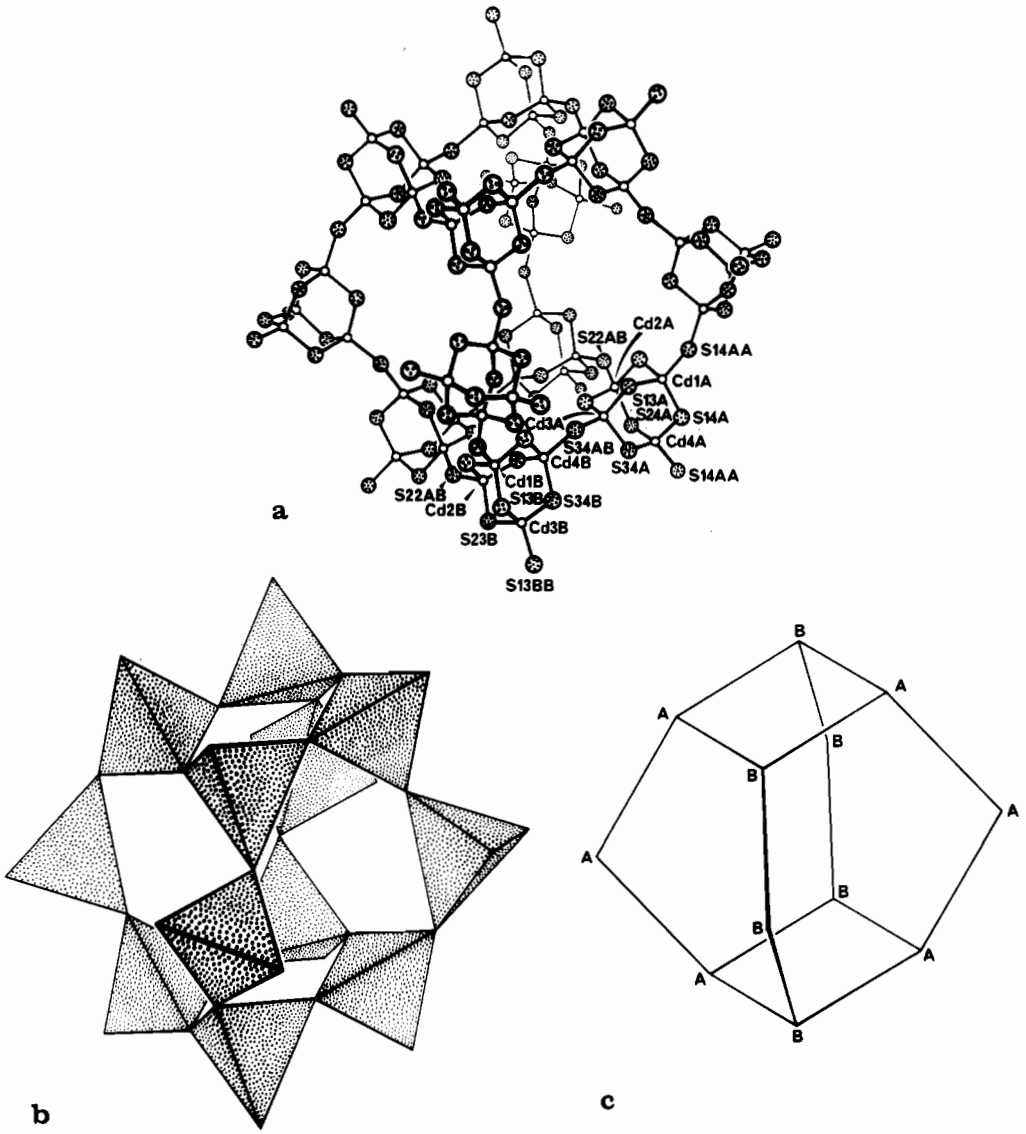


**Figure 5.** Drawings of an isolated cage of 12 adamantanoid tetrahedra in **3**, drawn to show (a) the Cd and S atoms, (b) the vertex-linked adamantanoid tetrahedra, and (c) the bitruncated octahedron created by the centroids of the adamantanoid tetrahedra. In part a S atoms are labeled with the symbols of the Cd atoms that they bridge. All Cd atoms and inter-adamantanoid cage S atom labels are marked, as are some intracage S atom labels.

relatively small differences in the orientations of the substituents (see Figure 2). Each of the four-membered rings of tetrahedra is centrosymmetric, with alternating A and B tetrahedra, while the six-membered rings are

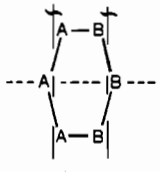


cycles that are folded about the diagonal marked and cycles in which the tetrahedra of the same type are related by the $2_1$ operations. The 12-vertex polyhedral cavity created by the adamantanoid tetrahedra has the topology of a trans bitruncated octahedron (see Figure 5c). There are 10 planar faces but only 16 edges (instead of the 20 for a bitruncated octahedron) because the equatorial edges (which are the fold-diagonals of the six-membered rings) are not connections between adamantanoid tetrahedra. There are eight A–B edges, four A–A edges, and four B–B edges.

The crystal lattice is generated from these cavity units by a stacking of them along *b*, with sharing of the four-membered-ring ABAB faces. These stacks are repeated in directions parallel to and approximately perpendicular to *c* and are linked to each other through sharing of the A–A and B–B edges in the six-membered rings. This is shown in the central part of Figure 6.

A consequence of the edge-sharing of the cavities is that they are not close-packed. There exist channels parallel to *b* between the cavities, as outlined on the sides of Figure 6. The walls of these channels are formed by the six-membered rings with their fold diagonals toward the axis of the channels. Inversion centers repeat at intervals of $b/2$ along the channels. The shortest connections around the channels are puckered eight-membered rings, which can be recognized in extended (chair) and folded (boat) conformations. The six-membered rings of each cavity provide openings between the center of the cavity and the four channels that surround each cavity. The stacks of cavities and the channels between them project as a square network along *b*.

The 12 adamantanoid tetrahedra that bound the cavity present eight triangular faces (around the four-membered rings) and four edges (connecting the four-membered rings) to the center of the cavity. Figure 7 shows the orientations of these boundary planes and edges and the relevant atom labels and symmetry operations. At the level of the individual $CdS_4$ tetrahedra, which form the internal surface of the cavity, there are 44 S atoms, connected by 32 Cd atoms. Figure 8 is a Schlegel diagram of the connections of the internal cavity surface showing the triangular faces and the four- and six-membered ring openings in the surface.

The large size of the cavity cage is revealed by the S---S distances shown in Figure 7; S---S diagonals through the inversion

**Table IV.** Cd–S Bond Distances for **2** and **3**.

| **2** | | **3** | | | |
|---|---|---|---|---|---|
| Cd(1)–S(1) | 2.539 (3) | Cd(1A)–S(12A) | 2.559 (3) | Cd(1B)–S(12B) | 2.561 (3) |
| Cd(1)–S(12) | 2.560 (3) | Cd(1A)–S(13A) | 2.562 (3) | Cd(1B)–S(13B) | 2.543 (3) |
| Cd(1)–S(13) | 2.528 (2) | Cd(1A)–S(14A) | 2.558 (3) | Cd(1B)–S(14B) | 2.536 (3) |
| Cd(1)–S(14) | 2.536 (2) | Cd(1A)–S(14AA) | 2.544 (3) | Cd(1B)–S(13BB) | 2.554 (3) |
| Cd(2)–S(2) | 2.519 (3) | Cd(2A)–S(12A) | 2.546 (3) | Cd(2B)–S(12B) | 2.509 (3) |
| Cd(2)–S(12) | 2.550 (3) | Cd(2A)–S(23A) | 2.538 (3) | Cd(2B)–S(23B) | 2.562 (3) |
| Cd(2)–S(23) | 2.547 (3) | Cd(2A)–S(24A) | 2.548 (3) | Cd(2B)–S(24B) | 2.532 (3) |
| Cd(2)–S(24) | 2.558 (3) | Cd(2A)–S(22AB) | 2.546 (3) | Cd(2B)–S(22AB)[c] | 2.528 (3) |
| Cd(3)–S(13) | 2.540 (3) | Cd(3A)–S(13A) | 2.545 (3) | Cd(3B)–S(13B) | 2.548 (3) |
| Cd(3)–S(23) | 2.546 (3) | Cd(3A)–S(23A) | 2.536 (3) | Cd(3B)–S(23B) | 2.572 (3) |
| Cd(3)–S(34) | 2.512 (3) | Cd(3A)–S(34A) | 2.537 (3) | Cd(3B)–S(34B) | 2.533 (3) |
| Cd(3)–S(2)[a] | 2.526 (2) | Cd(3A)–S(34AB) | 2.529 (3) | Cd(3B)–S(13BB)[d] | 2.557 (3) |
| Cd(4)–S(14) | 2.554 (2) | Cd(4A)–S(14A) | 2.534 (3) | Cd(4B)–S(14B) | 2.559 (3) |
| Cd(4)–S(24) | 2.530 (2) | Cd(4A)–S(24A) | 2.519 (3) | Cd(4B)–S(24B) | 2.517 (3) |
| Cd(4)–S(34) | 2.534 (2) | Cd(4A)–S(34A) | 2.569 (3) | Cd(4B)–S(34B) | 2.551 (3) |
| Cd(4)–S(1)[b] | 2.533 (3) | Cd(4A)–S(14AA)[e] | 2.543 (3) | Cd(4B)–S(34AB) | 2.549 (3) |

[a] $1-x, -^1/_2+y, ^1/_2-z$. [b] $^1/_2+x, ^1/_2-y, 1-z$. [c] $1-x, 1-y, 1-z$. [d] $-x, -^1/_2+y, ^1/_2-z$. [e] $1-x, -^1/_2+y, ^3/_2-z$.

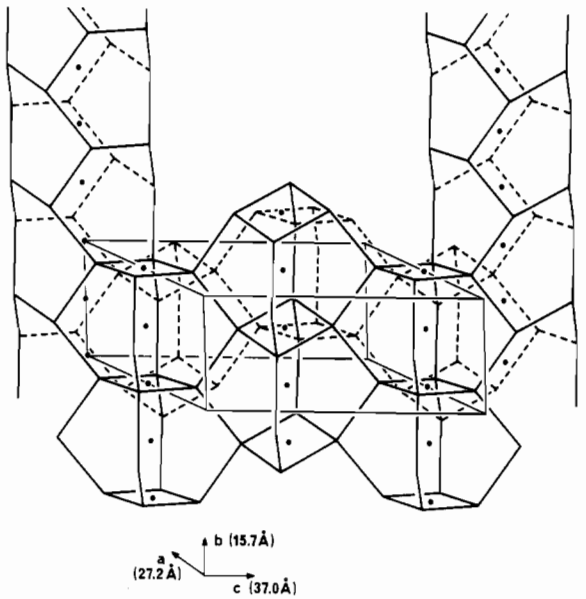


**Figure 6.** Lattice of **3**, drawn as the lines connecting the centroids of the adamantanoid tetrahedra that share vertices. Broken lines represent back connections, and dots represent centers of symmetry. The central part of the figure emphasizes the 12-vertex cavity-cage units, stacked along *b* through shared four-membered-ring faces, and linked parallel to and perpendicular to *c* by shared edges of six-membered rings. The left and right parts of the figure emphasize the channels that run between the stacks of the cavity-cage units. The $2_1$ axes parallel to *b* generate the continuous lines of edges shared between cavity cages.

center within the cavity range from 16.6 to 19.1 Å; S---S diagonals within the four-membered ring are 11.5, 12.0 Å, and the S---S diagonals of the six-membered ring are 11.1, 12.5, and 13.8 Å.

**Dimensions of Both Structures.** Selected bond distances at Cd and S are listed in Table IV, and all dimensions are included in the supplementary material. Intracage bridges are denoted $S^b$ and intercage bridges, $S^v$. In **2** the Cd–S distances range from 2.512 to 2.560 Å, mean ($\bar{x}$) 2.538 Å and *sample* standard deviation ($s$) = 0.013 Å,[15] while in **3** the corresponding values are as follows: range 2.509–2.572 Å, $\bar{x}$ = 2.545, and $s$ = 0.015 Å. In both structures there is no significant differentiation of intracage and intercage bond lengths. Range, $\bar{x}$, and $s$ values for $S^b$–Cd–$S^b$ angles are 100.2–122.1, 109.2, and 7.0° in **2** and 97.2–124.5, 108.8, and 9.2° in **3**; for $S^b$–Cd–$S^v$ angles, the corresponding values are 100.3–123.4, 109.6, and 6.5° in **2** and 96.9–126.0, 110.2, and 6.2° in **3**. As in other adamantanoid cage structures with SPh ligands, the intracage S–Cd–S angles are influenced sterically by the configurations of the two thiolate substituents involved.[2,16,17] The

(15) $s = [\sum_n (x-\bar{x})^2/(n-1)]^{1/2}$.

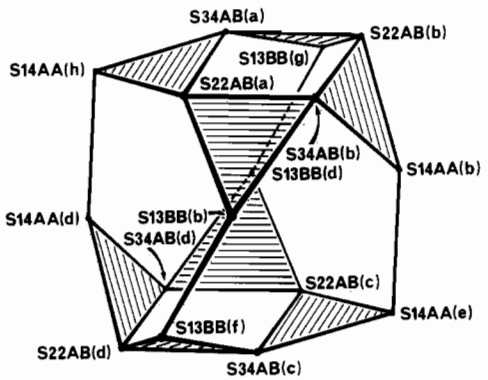


**Figure 7.** Triangular faces and edges of the adamantanoid tetrahedra that surround the polyhedral cavity in $Cd(SC_6H_4Me\text{-}4)_2$ (**3**). The symmetry operations are (a) $x, y, z$; (b) $1-x, 1-y, 1-z$; (c) $1-x, -y, 1-z$; (d) $x, y-1, z$; (e) $x, ^1/_2-y, z-^1/_2$; (f) $1+x, ^1/_2-y, ^1/_2+z$; (g) $-x, y-^1/_2, ^1/_2-z$; and (h) $1-x, y-^1/_2, ^3/_2-z$. S---S distances (Å): (i) through the inversion center within the cavity, $S(14AA)^b$---$S(14AA)^d$ 18.35, $S(13BB)^b$---$S(13BB)^d$ 19.13, $S(22AB)^a$---$S(22AB)^c$ 16.63, $S(34AB)^a$---$S(34AB)^c$ 18.57; (ii) across the center of inversion within the four-membered ring, $S(34AB)^a$---$S(34AB)^b$ 11.48, $S(22AB)^a$---$S(22AB)^b$ 12.04; (iii) across the six-membered ring: $S(14AA)^d$---$S(22AB)^a$ 11.10, $S(14AA)^d$---$S(13BB)^f$ 12.48, $S(14AA)^d$---$S(13BB)^b$ 13.82.

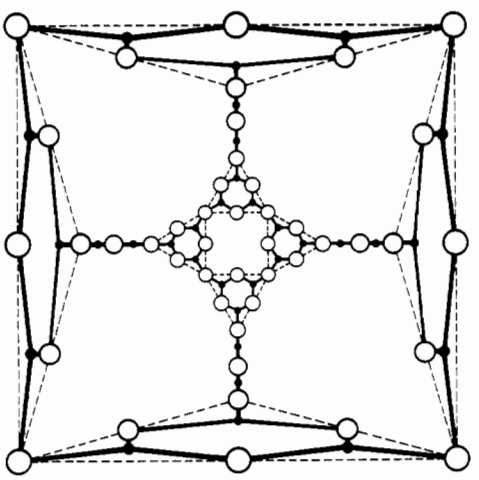

**Figure 8.** Schlegel diagram of the *connectivity* of the 32 Cd atoms (small filled circles) and 44 S atoms (larger open circles) on the internal surface of the cage in **3**. The triangular faces of eight adamantanoid tetrahedra are outlined with dotted lines; the other four adamantanoid tetrahedra appear only as their edges. One four-membered ring of the cage is the large outer square, the other is the small square at the center of the diagram, and the four six-membered rings of adamantanoid tetrahedra appear in the four quadrants. This diagram may be regarded as a perspective view into the cage through one four-membered ring window.

substituent configurations are axial (a) or equatorial (e) relative to the $Cd_3(\mu\text{-}SPh)_3$ cycles in chair conformation, and the configurational isomer of the $(\mu\text{-}SPh)_6Cd_4$ core of the cage is denoted by the distribution of substituents around each of the four fused cycles. In **2** the cage isomer is [aae, aae, aee, aee], while in **3** both cages are the isomer [aaa, aee, aee, aee]. Statistical analyses[15] of the S–Cd–S angles grouped according to the a/e configurations of the flanking substituents yield

| | **3** | **2** |
|---|---|---|
| a–a substituents, $\bar{x}$ ($s$) | 120.4° (2.8°) | 120.8° (1.4°) |
| a–e substituents, $\bar{x}$ ($s$) | 108.8° (5.0°) | 108.4° (4.4°) |
| e–e substituents, $\bar{x}$ ($s$) | 97.3° (2.5°) | 101.1° (0.9°) |

A significant feature of both structures is a differentiation of the Cd–S–Cd angles at *inter*cage and *intra*cage bridges, the former being substantially larger than the normal tetrahedral angles. Values of range, $\bar{x}$, and $s$ for $Cd\text{–}S^{v}\text{–}Cd$ are 132.7–139.5, 136.1, and 3.4° and 144.4–146.1, 145.2, and 0.8°, for **2** and **3** respectively, while the $Cd\text{–}S^{b}\text{–}Cd$ values are 104.9–112.0, 108.9, and 2.7 and 104.0–113.3, 109.4, and 2.7° for **2** and **3** respectively. There is definite correlation between the size of the Cd–S–Cd angle $\theta$ and the degree of pyramidality at the sulfur atom of the bridging thiolate: the latter is expressed as the out-of-plane angle $\phi$ between the S–C vector and the CdSCd plane. At the opened *inter*cage bridges, $\phi$ is 49.7 and 28.0° at the two $S^{V}$ atoms where $\theta$ is 133 and 140° in **2**, while in **3** the $\phi$ values are 49.7, 27.6, 38.5, and 36.2° for $\theta$ ranging from 144.8 to 146.1° at $S^{V}$. At the *intra*cage bridges, the $\phi$ populations in **2** and **3**, respectively, have means and sample standard deviations of 61.9 and 4.9° and 59.0 and 3.7°. Thus the increase in Cd–S–Cd at the intercage bridges by ca 30° correlates with a decrease in the S–C out-of-plane angle by values ranging from 10 to 30°. Correlations of this type are observed in other systems,[2,18] including **1**.

The centroid–centroid distances are almost invariant in **3**: the four independent distances are 9.72, 9.74, 9.76, and 9.81 Å. This is a manifestation of the constancy of the intracage Cd–S–Cd angles. These Cd–S–Cd angles are as follows: S(14AA), 146.1; S(22AB), 144.8; S(34AB), 144.4; S(13BB), 145.6; mean 145.2°, $s$ = 0.8°. They are closely comparable with the mean of average T–O–T angles for 14 zeolites,[19] namely 145°, $s$ = 6°.

**Packing of Thiolate Substituents in the Crystal Lattices. Structure 2.** The phenyl substituents at the intercage bridges lie close to the *bc* plane, and to the [011] direction, and do not point toward the pseudo fourfold screw axis. Of the intracage ligands, four (per *c* repeat) are directed into the space around the pseudo fourfold screw axis and are approximately perpendicular to it, while four others are approximately tangential to this space and thus positioned roughly between adamantanoid cages repeating along *c*. Four other intracage ligand substituents are directed into the space around the $2_1$ axes parallel to *c*.

**Structure 3.** The dispositions of the 4-methylphenyl substituents in the lattice of **3** are analyzed in terms of the major available volumes, namely the cavities and the extended channels. Individual substituents can be classified[20] (i) as protruding into the cavity, (ii) as protruding into the channel, or (iii) as lying approximately tangential to the boundaries between the cavities and the channels.

We describe first the *10* substituents that occupy the cavity cage, a number which is less than one-fourth of the 44 ligand S atoms that constitute the boundary of the cavity cage. Figure 9 provides details. There are 24 intra-adamantanoid bridging ligands on the triangular faces of the cavity (see Figure 7), but because these faces have the [aee] substituent configuration, only eight ligands

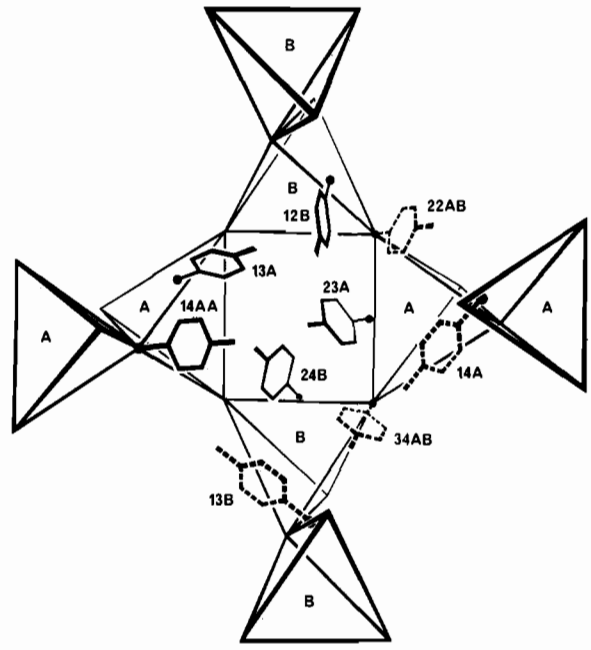


**Figure 9.** Representation of the adamantanoid tetrahedra that surround the cavity in **3** and of the 4-methylbenzenethiolate ligands that are located in or near the cavity. For clarity, the four adamantanoid tetrahedra of the top four-membered ring have been omitted, as have ligands related by inversion through the center of the cavity. The five independent ligands that protrude into the cavity are drawn with solid lines; those four that are approximately tangential to the surface of the cavity are drawn with broken lines.

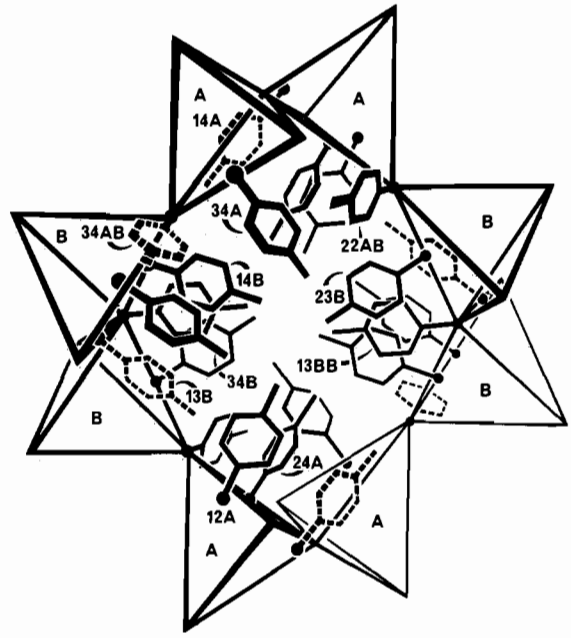


**Figure 10.** Representation of the ligands on a centrosymmetric eight-membered ring of adamantanoid tetrahedra surrounding the channel in the crystal structure of **3**. The 4-methylbenzenethiolate ligands that protrude into the channel are drawn with solid lines, and those tangential to the channel are drawn with broken lines.

(13A, 12B, 23A, 24B, and their equivalents due to the center of symmetry) protrude into the cavity. There are eight inter-adamantanoid-bridging ligands around the four-membered rings (22AB, 34AB, and equivalents), all of which are tangential to the cavity walls with four only associated with any one cavity. The edges around the central belt of the cavity contribute four intra-adamantanoid ligands (14A, 13B, and equivalents), all of which are tangential to the cavity boundaries, and eight inter-adamantanoid ligands that connect to the triangular faces, of which one pair (14AA and its centrosymmetric equivalent) protrude directly

(16) Dance, I. G.; Choy, A.; Scudder, M. L. *J. Am. Chem. Soc.* **1984**, *106*, 6285.
(17) Dance, I. G.; Bowmaker, G. A.; Clark, G. R.; Seadon, J. K. *Polyhedron* **1983**, *2*, 1031.
(18) Dance, I. G.; Fitzpatrick, L. J.; Scudder, M. L. *J. Chem. Soc., Chem. Commun.* **1983**, 546.
(19) Barrer, R. M. *Zeolites and Clay Minerals as Sorbents and Molecular Sieves*; Academic: New York, 1978; p 97.
(20) Considering only the S···Me vector of each ligand, not the rotational conformation of the ligand plane.

into the cavity. The methyl carbon atoms of two ligands 23A are in van der Waals contact (3.5 Å) across the center of the cavity cage; the methyl carbon atoms of ligands 14AA and 12B are 3.39 and 3.89 Å, respectively, from the center of the cavity.

The [aaa] faces of the adamantanoid tetrahedra are directed toward the channels, and consequently a larger number of ligand substituents are within the channels. Figure 10 shows the ligands associated with a centrosymmetric eight-membered ring that surrounds the channel. Intra-adamantanoid ligands 12A, 24A, 34A, 14B, 23B, and 34B and the inter-adamantanoid ligand 13BB protrude directly into the channel, while ligands 14A, 13B, 22AB, and 34AB are approximately tangential to the walls of the channel. Along the channel, the methyl carbon atoms of ligands 14B and 34A are 2.78 and 2.96 Å, respectively, from the center of symmetry at $z = {}^1/_2$, and the methyl carbon atoms of ligands 13BB and 23B are 2.74 and 3.10 Å from the center of symmetry at $z = 0$.

Our measurements of the $^{113}Cd$ and $^{13}C$ NMR spectra of DMF solutions of **2** and **3**, and the interpretations in terms of molecular aggregates in temperature-dependent equilibria, will be reported separately.

## Discussion

The structures of **2** and **3** are the first reported three-dimensionally nonmolecular crystal structures for homoleptic metal thiolates. They refute the forecast[2] that three-dimensionally nonmolecular structures are unlikely for metal thiolates with all but the smallest substituents. The revised structural principle to be extracted from these results is that an enlarged (145°) Cd–S–Cd angle occurs generally at doubly bridging thiolate ligands linking adamantanoid cages, with the consequence that open arrays of adamantanoid cages can occur. The crystal structures of **2** and **3** are also the first reported for any compound with adamantanoid cages vertex-linked infinitely in *three* dimensions. Two-dimensionally nonmolecular polyadamantanoid structures occur in the metal chalcogenides $KInSe_2$,[21] $TlGaSe_2$,[21,22] and $Ag_3B_5S_9$.[21] In **3** very large cages are constructed from smaller adamantanoid cages. Two types of polyadamantanoid aggregate are now known, those in which the adamantanoid cages are fused and those in which they are vertex-linked; we differentiate these two types with the compound adjectives "poly-fused-adamantanoid" and "poly-linked-adamantanoid".

The replacement of hydrogen by methyl at the 4-position on the benzenethiolate ligand causes a fundamental change in the linkage patterns of the adamantanoid tetrahedra. In **2** the framework does not contain closed cycles of tetrahedra, whereas in **3** there are four-, six-, and eight-membered closed cycles, which result in a framework containing larger centrosymmetric cavities, akin to the aluminosilicate frameworks. We have previously pointed out that the structures of some metal–sulfide–thiolate complexes are molecular fragments of nonmolecular metal sulfide structures.[2] This theme of structural congruence is reappearing here in the form of structural similarities between metal thiolates and oxo–metal lattices.

It is interesting to explore further the analogy between the structures of the $M(SAr)_2$ compounds and the zeolite aluminosilicates, by assessing the relative volumes of the framework tetrahedra in the lattices. The volumes of the adamantanoid tetrahedra, calculated from the internuclear edge vectors, are 65.4 $Å^3$ in **2** and 65.8 (A) and 67.0 (B) $Å^3$ in **3**. These volumes are those of a regular tetrahedron of edge length 8.2 Å. The volume excluded by these tetrahedra is calculated by addition of 3.6 Å (ca. twice the van der Waals radius of S) to the edge length, yielding $V^{tet} = 150$ $Å^3$. From this it is calculated that the total volumes excluded by the adamantanoid tetrahedra are 12% and 10% of the unit cell volumes in **2** and **3** respectively. Application of the same calculation to the $TO_4$ (T = Si, Al) tetrahedra of typical zeolites by using 2.70 Å internuclear edge length plus two 1.5-Å van der Waals radii, leads to total volumes excluded by the $TO_4$ tetrahedra on the order of 22% (in sodalite), 31% (zeolite A), and 39% (faujasite) of the total cell volume.[23,24] It is evident that the Cd,S framework that maintains the lattice structure in **2** and **3** occupies a *lesser* proportion of the crystal volume than the aluminosilicate frameworks in zeolites. Distribution of the remaining unexcluded volumes (88% and 90% of the cell volumes) among the substituents of **2** and **3**, respectively, yields volumes of 139 $Å^3$ for $C_6H_5$ in **2** and 165 $Å^3$ for $C_6H_4Me$ in **3**. Comparison with the volume per molecule in crystalline benzene, 127 $Å^3$, indicates that the cavities in **2** are not filled.

**Acknowledgment.** Funding by the Australian Research Grants Scheme is gratefully acknowledged. We thank Dr. A. D. Rae for assistance with the program RAELS.

**Registry No.** $Cd(SPh)_2$, 21094-83-7; $Cd(SC_6H_4Me\text{-}4)_2$, 110662-12-9.

**Supplementary Material Available:** Table IS, giving all atomic coordinates, thermal parameters, and bond distances and angles for **2**, Table IIS, giving all atomic coordinates, thermal parameters, and bond distances and angles for **3**, Table IIIS, giving correlation of out-of-plane angles $\phi$ and bond angles $\theta$ at bridging thiolate ligands in structure **2**, Table IVS, giving correlation of out-of-plane angles $\phi$ and bond angles $\theta$ at bridging thiolate ligands in structure **3**, Table VS, giving powder diffraction data for **2**, and Table VIS, giving powder diffraction data for **3** (15 pages); Table VIIS, giving structure factors for **2**, and Table VIIIS, giving structure factors for **3** (58 pages). Ordering information is given on any current masthead page.

(21) Krebs, B. *Angew. Chem., Int. Ed. Engl.* **1983**, *22*, 113.
(22) Muller, D.; Hahn, H. *Z. Anorg. Allg. Chem.* **1978**, *438*, 258.
(23) Data from ref 19.
(24) An alternative measure of the porosity of the zeolites is obtained from the volume of water released during the preparative dehydration: this free volume ranges from 20% to 50% of the total.[19]